

A new algorithm for the analysis of strange attractors

Octaviana Datcu, Roger Tauleigne, Jean-Pierre Barbot

► **To cite this version:**

Octaviana Datcu, Roger Tauleigne, Jean-Pierre Barbot. A new algorithm for the analysis of strange attractors. International Symposium on Signals, Circuits and Systems (ISSCS), Jul 2013, Iasi, Romania. 2013. <hal-00923697>

HAL Id: hal-00923697

<https://hal.inria.fr/hal-00923697>

Submitted on 3 Jan 2014

HAL is a multi-disciplinary open access archive for the deposit and dissemination of scientific research documents, whether they are published or not. The documents may come from teaching and research institutions in France or abroad, or from public or private research centers.

L'archive ouverte pluridisciplinaire **HAL**, est destinée au dépôt et à la diffusion de documents scientifiques de niveau recherche, publiés ou non, émanant des établissements d'enseignement et de recherche français ou étrangers, des laboratoires publics ou privés.

A new algorithm for the analysis of strange attractors

Octaviana Datcu¹, Roger Tauleigne², Jean-Pierre Barbot³

¹ ETTI, Politehnica University of Bucharest, Roumania

octavianadatcu@yahoo.com,

² CNAM, 292 rue Saint Martin, 75003, Paris, France

tauleigne@ensea.fr

³ ENSEA, 6 Avenue du Ponceau, 95014, Cergy-Pontoise, France

barbot@ensea.fr

Abstract— This work proposes a new algorithm aiming to locally measure the divergence of initially nearby trajectories. The divergence is considered in the case of strange attractors, as an alternative of classical Lyapunov exponents. The new algorithm makes use of the Euclidean distance in order to define the local divergence. It is, then, possible to analyze the geometry of the attractor through layers of same divergence, such as a tomography. The algorithm is applied, as an example, to the Colpitts chaotic oscillator.

I. INTRODUCTION

The sensibility to initial conditions Lorenz had discovered, as described in [1], has quickly led to the exhibition of complex attractors which included rapidly divergent areas joint with contraction zones. Guided by a low dimensional dynamics, the trajectory of the system successively sweeps a stretching area followed by a folding zone. The Baker's map, [2], or Smale's Horseshoe map, [3], are typical examples of simple recurrence relations that produce strange attractors.

The topology of these behaviors is nowadays much more studied, as, for example, in [4] or [5]. Nevertheless, our purpose is not to prolong these works, but to bring along a tool for the local analysis of the use of chaotic behavior.

We propose an algorithm capable of classifying all the points of the attractor depending of the intensity of the divergence, which can as well be negative (i.e. convergence). This particularity of the analysis appears to us as a pertinent tool for the use of chaotic systems in the encryption of data flows. These applications exploit a physical phenomenon a priori surprising, the synchronization of chaotic signals. As two persons who march together synchronize their steps, two chaotic identical systems synchronize their states, when they fulfill the condition to communicate, even partially, as shown in [6].

The robustness of this synchronization allows the superposition of a message to this communication, as well as its extraction by the synchronized receiver. In order to render the identification more difficult to an eavesdropper, it seems pertinent to include the message while the trajectory of the states of the transmitter passes by a divergent area. These is why our work, which differentiate among convergent, slow divergent and fast divergent areas of the attractor, has a solid argument to be done.

Remark on the Lyapunov exponents

In order to demonstrate the chaotic behavior of an attractor, the most used criterion is the divergence rate of two trajectories initialized with nearby values. As this divergence is caused by the structure of the equations, it is logical to suppose a cumulative effect, which leads to an exponential progression of the divergence. We take, here, Lyapunov's assumptions, which in the one-dimensional case are formalized as follows:

Let $f^n(x)$ be a monodromy from \mathfrak{X} to \mathfrak{X} which leads x_i into x_{i+1} . Let us choose two initial conditions separated by a very small ε , x_0 and $x_0 + \varepsilon$, and observe how the distance between the two trajectories behaves.

$$\varepsilon \cdot e^{n\lambda(x_0)} = |f^n(x_0 + \varepsilon) - f^n(x_0)| \quad (1)$$

The Lyapunov exponent resumes this behavior to only one value, depending of the initial condition:

$$\lambda(x_0) = \frac{1}{n} \ln \left(\left| \frac{f^n(x_0 + \varepsilon) - f^n(x_0)}{\varepsilon} \right| \right) \quad (2)$$

After passing to the limit, on can obtain (3), and consequently, (4).

$$\lambda(x_0) = \lim_{n \rightarrow \infty} \lim_{\varepsilon \rightarrow 0} \frac{1}{n} \ln \left(\left| \frac{f^n(x_0 + \varepsilon) - f^n(x_0)}{\varepsilon} \right| \right) \quad (3)$$

$$\lambda(x_0) = \lim_{n \rightarrow \infty} \frac{1}{n} \ln \left| \frac{df^n(x_0)}{dx} \right|, \quad (4)$$

with

$$\frac{df^n(x_0)}{dx} = f'(x_{n-1}) \cdot f'(x_{n-2}) \dots f'(x_1) \cdot f'(x_0) \quad (5)$$

This eventually leads to the expression in (6) for the Lyapunov exponent.

$$\lambda(x_0) = \lim_{n \rightarrow \infty} \frac{1}{n} \sum_{i=0}^{n-1} \ln \left| \frac{df^n(x_0)}{dx} \right| \quad (6)$$

When reducing the number of the terms of this series, we can obtain a local measure of the sensibility to initial conditions. A good such an algorithm, which allows the computation of the Lyapunov exponents from time series, is [8]. When these computations are done, the distance between two trajectories is replaced by the derivative of the initial distance between them. Thus, the Lyapunov exponent does not provide the local value of this distance.

The Lyapunov exponents describe the projection of the sensitivity to initial conditions for each direction indicated by the axis of the phase space. This sensitivity does not merely mean that the two reference trajectories diverge effectively at each moment, but that they are diverging in average.

Consequently, we propose measuring the Euclidean distance between the evolutions of the two reference trajectories, this quantity describing the real instantaneous distance between two points of the trajectory.

II. MEASURING THE DIVERGENCE BY THE EUCLIDEAN DISTANCE

The alternation dilatation/compression of the flow is a necessary characteristic to a chaotic attractor bounded by principle. Consequently, the same trajectory revisits the vicinity of a point of the phase space it already filled.

It is, then, possible to choose two nearby points $x_A = (x_1(n), x_2(n), x_3(n))$ and $x_B = (x_1(m), x_2(m), x_3(m))$ with $m > n$, measure the distance between them, tracking the evolution of this distance. Thereby, we obtain a measure of the divergence (convergence). The Euclidean distance is expressed by (7).

$$d_{AB}(m) = \sqrt{\sum_{i=1,3} (x_i(m) - x_i(n))^2} \quad (7)$$

The proposed method is applied, as an example, on the chaotic Colpitts oscillator, three dimensional system described by (8). For a detailed analysis of the Colpitts chaotic oscillator, see [8].

$$\begin{aligned} \dot{x}_1 &= -I_S e^{-x_2/V_T} / C_2 + x_3 \\ \dot{x}_2 &= (-I_0 + x_3) / C_2 \\ \dot{x}_3 &= (x_1 + x_2) / L - R_1 x_3 / L + V_1 \end{aligned} \quad (8)$$

We use parameters $g=4.46$, $Q=1.38$, $k=0.5$, and initial conditions $x_1=0.6787$, $x_2=0.7577$, $x_3=0.7431$, for our exemplification.

When considering a large number of iterations, one can observe, in Fig. 1, the grate dynamics of the Euclidean distance, from 1 to 67, its great irregularity illustrating the chaotic nature of this attractor. This figure shows the existence of extremely localized great divergences.

A zoom on the evolution illustrated in Fig. 1, allows estimating the value of the rate of a great excursion, as in Fig. 2. The computation step is considered to be 10^{-3} .

The Euclidean distance at iteration 31720 is $d_1=3.376$, and at iteration 32490 is $d_2=64.58$, being amplified with approximately 1812% during 770 steps. This ascertainment, which is applicable to a great number of similar transitions, justifies a local analysis of the divergence through the measurement of Euclidean distances.

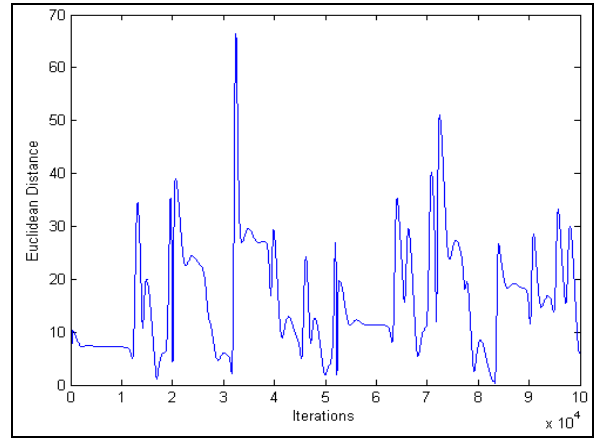


Figure 1. Evolution of the Euclidean distance (box number 404).

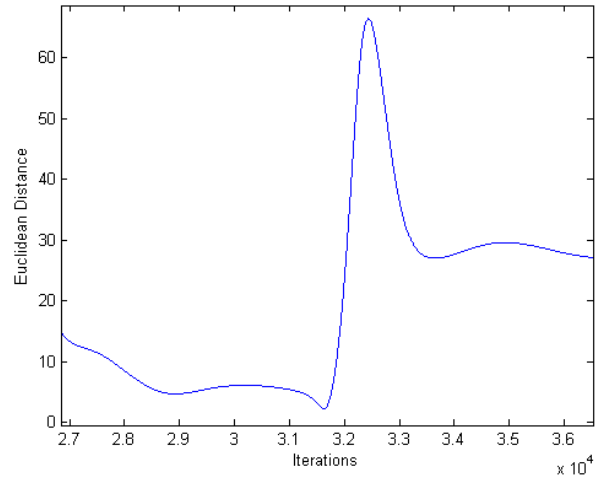


Figure 2. Evolution of the Euclidean distance (box number 404). Zoom.

III. APPLICATION TO LOCAL ANALYSIS

A. Description of the algorithm

Let $F(x_i)$ with $i=1, \dots, n$ be a dynamical nonlinear system. Let $X=(x_1, x_2, \dots, x_n)$ be its state vector. The dynamics of this system spreads within a n -dimensional phase space. On each direction of the state vector, the dynamics is bounded by x_i^{min} and x_i^{max} , implying $\Delta x_i = x_i^{max} - x_i^{min}$, for all $i=1, \dots, n$.

All the intervals Δx_i are partitioned in p δ_i -length segments. The conjunction of these divisions builds in the phase space cubic boxes. They completely pave the space filled by the strange attractor.

The boxes are indexed with the b value as in Table I.

While the trajectory of the state vector intersects a box, its position (number of iterations) is stored. This is the first point considered for the computation of the Euclidean distance, $(x_A(i)=(x_1(i), x_2(i), x_3(i)))$. While the trajectory revisits the same box, its position is stored again, and it defines the second point, $(x_A(j)=(x_1(j), x_2(j), x_3(j)))$. The distance at the entrance of the considered box is given in (9).

$$d_{in} = x_A(i) - x_B(j) \quad (9)$$

| b | x_1 | x_2 | \dots, x_{n-1} | x_n |
|-------|-------------|-------------|--|-------------------------|
| 1 | $x_1(\min)$ | $x_2(\min)$ | $\dots, x_{n-1}(\min)$ | $x_n(\min)$ |
| 2 | $x_1(\min)$ | $x_2(\min)$ | $\dots, x_{n-1}(\min)$ | $x_n(\min + \delta_n)$ |
| 3 | $x_1(\min)$ | $x_2(\min)$ | $\dots, x_{n-1}(\min)$ | $x_n(\min + 2\delta_n)$ |
| ... | | | | |
| p | $x_1(\min)$ | $x_2(\min)$ | $\dots, x_{n-1}(\min)$ | $x_n(\max - \delta_n)$ |
| $p+1$ | $x_1(\min)$ | $x_2(\min)$ | $\dots, x_{n-1}(\min + \delta_{n-1})$ | $x_n(\max - \delta_n)$ |
| $p+2$ | $x_1(\min)$ | $x_2(\min)$ | $\dots, x_{n-1}(\min + 2\delta_{n-1})$ | $x_n(\max - \delta_n)$ |
| ... | | | | |

After k calculus steps, we measure the Euclidean distance between the evolution of the two initial points, as in (10).

$$d_{out} = x_A(i+k) - x_B(j+k) \quad (10)$$

Thereafter, we quantify the divergence observed within this box by the rate $D(b)$, defined by (11), where b is the number of the box.

$$D(b) = (d_{out} - d_{in}) / d_{in} \quad (11)$$

B. Convention

A positive value of the rate $D(b)$ means an increasing distance between the two trajectories, i.e. a local divergence. While the two trajectories locally converge, $D(b)$ becomes negative and we name it a negative divergence.

C. Exemplification on a chaotic Colpitts oscillator

As in the previous paragraph, we use the chaotic Colpitts oscillator to illustrate our algorithm. Consequently, we have $n=3$, the number of states of the system, the number of iterations within each box is set to $k=100$. The partition of the phase space is illustrated in Fig. 3, where only the boxes which intersect the trajectory of the system are shown.

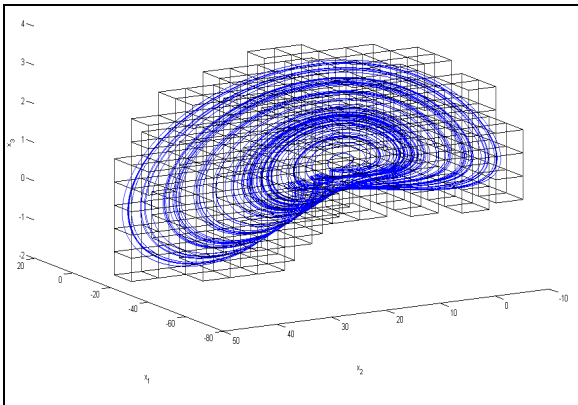


Figure 3. Partition of the phase space (x_1, x_2, x_3) of the Colpitts attractor.

The Euclidean distance between two successive entries of the trajectory in the same box is not constant within this box. The

figures below show different possible evolutions of the Euclidean distance between initially considered entry points. The values of the divergence $D(b)$ are very different and the emphasize the local nature of our measurements.

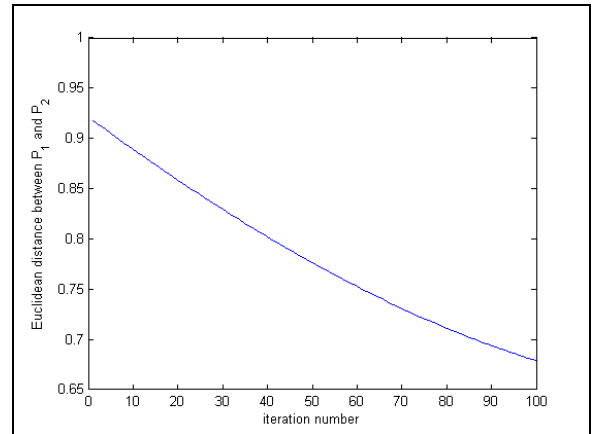


Figure 4. Convergence example : $D(783) = -3,1.10^{-3}$ (box n° 783).

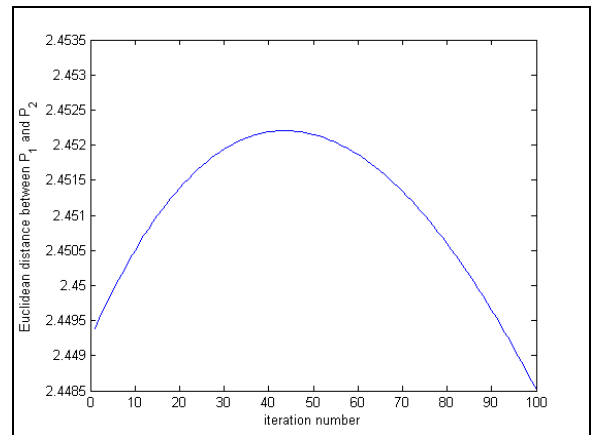


Figure 5. Within box n°19 ($D(19) = 4.10^{-4}$).

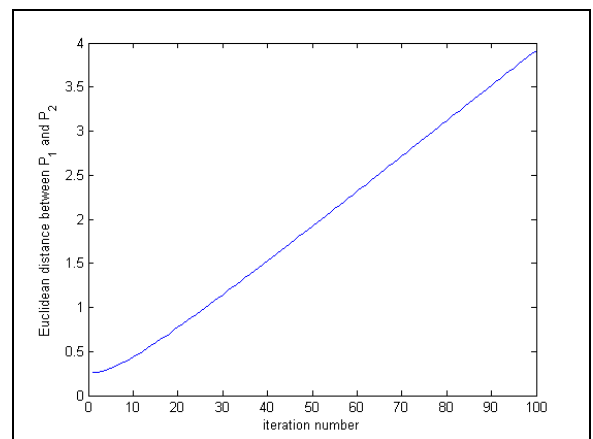


Figure 6. Great divergence example : $D(304) = 3,3.10^{-3}$ (box n° 304).

IV. TOMOGRAPHY

To formulate the analysis of all the boxes, we can use statistical tools, but it is much more efficient to trace cartography in the phase space. We replace the trajectories by the value of the divergence in each box. We discover, then, a new geometry of the attractor, throughout this tomography. The use of the medical term in this context is done because there are considered intervals of values of the divergence, the dynamics of the divergence partitions the strange attractor by layers.

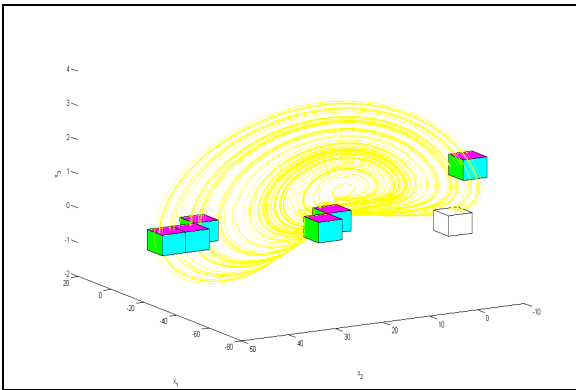


Figure 7. Tomography of convergent areas.

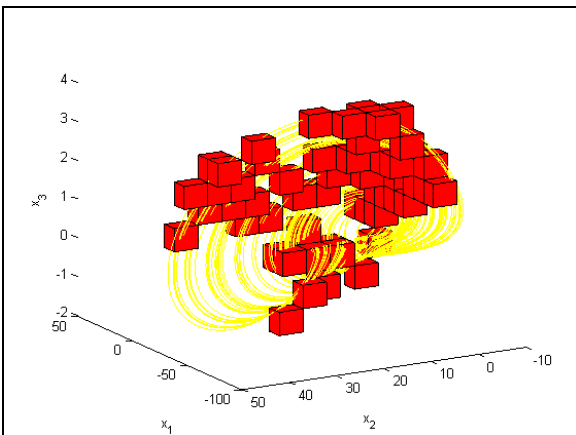


Figure 8. Tomography of low contraction areas.

V. CONCLUSIONS

Our algorithm measures the real local divergence of chaotic attractors. The accuracy of this measurement is adjustable by the sampling step of state variables, which defines the size of the boxes. It is then possible to analyze the attractor from a given interval of divergence. Each interval forms a layer of the dynamics of divergence of the entire attractor. Graphically we can build a complete tomography of the attractor. It enables one to easily identify the sites of the attractor zones based on the value of the required divergence.

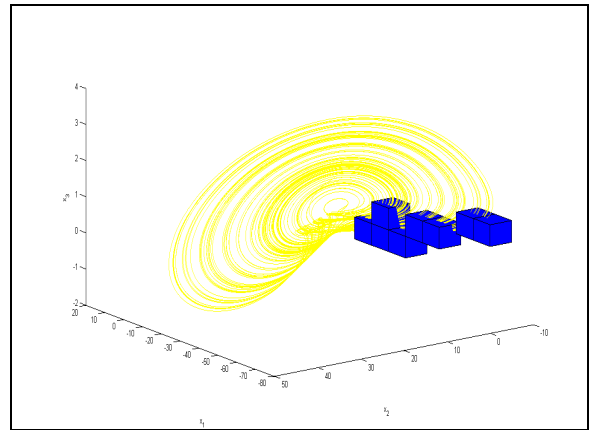


Figure 9 Zone de grande divergence.

REFERENCES

- [1] E. N. Lorenz, "Deterministic nonperiodic flow", Journal of Atmospheric Sciences, vol. 20, pp. 130-141.
- [2] R. J. Fox, "Construction of the Jordan basis of the Baker map", Chaos, 1997.
- [3] S. Smale, "Differentiable dynamical systems", Bulletin of the American Mathematical Society, vol. 73 (6), 1967, pp.747-817.
- [4] C. Letellier and L. A. Aguirre, "Interplay between synchronization, observability, and dynamics", Physical Review E, 82, 2010.
- [5] C. Letellier, J. Maquet, L. Le Scellery, G. Gouesbety and L. A. Aguirre, "On the non-equivalence of observables in phase-space reconstruction from recorded time series", J. Phys. A: Math. Gen. 31, Printed in the UK PII: S0305-4470(98)93312-1, 1998, pp. 7913-7927.
- [6] T. Stojanovski, L. Kocarev and U. Parliz, "Driving and synchronizing by chaotic impulses", Phys. Rev. E., vol. 54, no. 2, 1996, pp. 68-73.
- [7] A. Wolf, J. B. Swift, L. Swinney, and J. A. Vastano, "Determining Lyapunov exponents from a time series", Physica Journal, 1985, pp. 285-317.
- [8] O. de Feo, G. M. Maggio and M. P. Kennedy, "The Colpitts oscillator: families of periodic solutions and their bifurcations" Int. J. Bifurcation Chaos 10, 2000.